Performance Analysis of Hybrid-ARQ with Chase Combining over Cooperative Relay Network with Asymmetric Fading Channels

Yun Ai, Michael Cheffena
Norwegian University of Science and Technology, N-2815 Gjøvik, Norway
Email: {yun.ai, michael.cheffena}@ntnu.no

***Abstract*—This paper investigates the performance of cooperative relay networks in the presence of hybrid automatic repeat request (ARQ) with delay constraint. It analyzes the scenarios where the relay channels are asymmetric (i.e., the links of the wireless relay network follow different fading distributions) due to relaying position and/or due to time varying channel fading. The analytical expressions for the outage probability and throughput are derived for different asymmetric fading channels. The benefit of combined implementation of relaying and hybrid-ARQ is illustrated. Our results show that the performance in terms of outage probability and delay-limited throughput is better when the relay node is in line-of-sight (LoS) with respect to the source node compared to being close to the destination node. This performance difference is quantified and can be as large as several dB depending on the specific configuration. This difference in performance narrows when the maximum hybrid-ARQ transmission rounds increase or when the information transmission rate decreases.**

***Index Terms*—Hybrid automatic repeat request (ARQ), chase combining, cooperative network, relaying channels, asymmetric channels, outage probability, throughput analysis.**

I. Introduction

Over the last decades, wireless relay network has attracted huge interests from both the academia and industry thanks to its numerous benefits. By implementing intermediate relay nodes to support the data transmission from a source to a destination, it has been shown that a substantial increase in the multiplexing gain and spatial diversity of the communication systems can be achieved, which leads to improved network coverage and enhanced system throughput [1]. Depending on the nature and complexity of the relaying technique, relay strategies can be generally classified into two categories, namely decode-and-forward (DF) and amplify-and-forward (AF) [2, pp. 412–416].

The performance of relay-aided wireless network can be further improved by the combined implementation of the cooperative relaying technique in the physical layer and the hybrid automatic repeat request (hybrid-ARQ) scheme in the link layer [3]. The hybrid-ARQ is a well-established retransmission mechanism which has been employed in virtually all modern communication systems. It is usually categorized into Chase combining (CC) and incremental redundancy (IR), depending on whether the retransmission is identical to the original transmission or it consists of new redundancy bits from the channel encoder [2, pp. 96–101]. The ARQ systems can be interpreted as channels with sequential feedback, where the system performance can be improved by retransmitting data that has been impaired by unfavorable channel conditions through the use of both error correction and error detection codes. Therefore, the combination of the relaying and ARQ improves the system performance as the ARQ makes it possible to use the relay nodes only when it is needed [4]. This motives to study the performance of hybrid-ARQ technique in wireless relay networks [3]–[7].

In [3] and [4], outage probability and throughput analysis is conducted for an ARQ-enabled relay network. The authors assume a quasi-static block-fading channel condition, where the channel coefficients are assumed to remain fixed within all ARQ rounds of a data packet. This assumption only represents the limited scenarios with slow-moving or stationary nodes. In [5], the throughput and outage probability of a three-node relay network with hybrid-ARQ and long-run sum power constraint is analyzed. It is assumed that the source will stop transmission once the relay correctly decodes the data. While this eases the requirement on synchronization and interference management, the destination node cannot benefit from the diversity gain resulting from the cooperative transmission of both source and relay. The authors in [6] investigated the performance of multiple-input-multiple-output (MIMO) with ARQ and showed that the performance of ARQ with CC and IR are the same at low/moderate SNRs. The performance of an ARQ-enabled relay network with cooperation mode switch is analyzed in [7].

However, the aforementioned work, as well as the vast majority of related literature, limit their study of relay networks with hybrid-ARQ to symmetric fading channel conditions, i.e., all links follow the same distribution. In reality, an asymmetric fading channel is regarded as a more general and realistic assumption to describe the actual wireless relay channels considering the spatial variability of node locations as well as spatio-temporal dynamics of the propagation channel [8]–[10]. To this end, there have been some recent papers focusing on the performance of wireless network over asymmetric fading channels [8]–[10]. A dual-hop AF relaying system has been studied for asymmetric Rayleigh-Rician fading channels in [8] and for Rician-Nakagami-m case in [9]. The authors of [10] have investigated a dual-hop DF relaying network over mixed Rayleigh and generalized Gamma fading channels. The

analysis of wireless relay network over mixed fading channels is mathematically much more complicated for analysis compared to the scenario where all fading channels follow the same distribution. From the above up-to-dated reported works, it is fairly evident that the performance of relay network with hybrid-ARQ over asymmetric fading channels is still unexplored. In this paper, we intend to fill this gap.

In this paper, we study the performance of hybrid-ARQ with CC over a cooperative relay network with mixed Rayleigh and Rician fading channels. The closed-form expressions for the outage probability at each hybrid-ARQ round are derived and the delay-limited (DL) throughput of the network is analyzed. Fast-fading channel condition is adopted such that the channel coefficients change in each (re)transmission round based on their probability density functions (PDFs). The relay node employs the DF relaying strategy.

The remainder of the paper is organized as follows. In Section II, we describe the relay channel model with the hybrid-ARQ protocol. Performance analysis, including the outage probability is conducted in Section III, and throughput analysis in Section IV. The analytical and simulation results are presented in Section V. Section VI concludes the paper.

II. Relay-ARQ Protocol and Channel Model

We consider a cooperative communication setup consisting of a source node, a relay node and a destination node as shown in Fig. 1. The relay-ARQ protocol works as follows: during the first hybrid-ARQ round of each packet period, the source broadcasts the data to the destination node, which is also overheard by the relay node. At the end of transmission, the destination node feedbacks its decoding result to both the source and the relay using the acknowledgement (ACK) or non-acknowledgement (NACK) messages, which are assumed to be received error-free. If retransmissions are required and the relay correctly decodes the data before the destination, the relay and the source will cooperatively transmit the data to the destination. The space-time codes (STCs) such as Alamouti code are used to transmit the source and relay symbols in order to avoid interference. It should be noted that the decoding at both the relay and the destination benefits from the hybrid-ARQ mechanism. In addition, the decoding at the destination also benefits from the potential cooperative transmission of the source and the relay. Furthermore, we also assume a delay-limited network with maximum number of hybrid-ARQ transmission rounds M, representing the delay constraint.

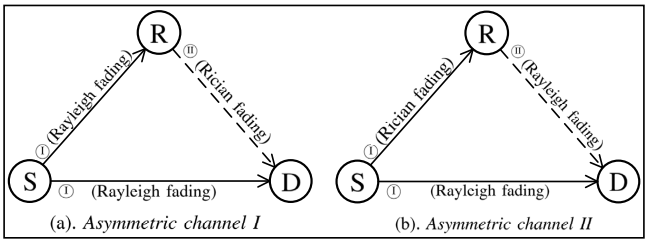

Fig. 1: The system model with asymmetric fading channels

The channel fading coefficients for the source-destination, source-relay, and relay-destination links are denoted as h_{sd}, h_{sr}, and h_{rd}, respectively. The corresponding fading distributions of each link are shown in Fig. 1 for the investigated asymmetric channels. For a wireless relay network (e.g. wireless sensor network), the positions of the transmitter (source node) and the receiver (destination node) are often fixed while the position of the relay is flexible. We assume that there is no line-of-sight (LoS) between source and destination. The relay may be placed close to either the destination or the source to have a LoS. In the former case, the source-relay link follows Rayleigh fading and the relay-destination link follows Rician fading. In the latter case, the source-relay link follows Rician fading and the relay-destination link follows Rayleigh fading. The two Rayleigh fading channels are independent but not necessarily identical. It is evident that the scenario of all links following Rayleigh distribution is a special case of our analysis. Let the transmission power of the source and the relay be P_s and P_r, respectively. The instantaneous SNRs for the three links are expressed as $\gamma_{sd} = (P_s|h_{sd}|^2)/N_0$, $\gamma_{sr} = (P_s|h_{sr}|^2)/N_0$, and $\gamma_{rd} = (P_r|h_{rd}|^2)/N_0$, where N_0 is the noise power. Their mean values are denoted as $\overline{\gamma}_{sd}$, $\overline{\gamma}_{sr}$, and $\overline{\gamma}_{rd}$, respectively. The input SNR of the system is defined as $\gamma' = (P_s + P_r)/N_0$.

For AWGN channel, if a link undergoes Rayleigh fading, the corresponding instantaneous SNR γ follows the exponential distribution. The PDF of the SNR is expressed as

$$f_\gamma(\gamma) = \frac{1}{\overline{\gamma}} e^{-\frac{\gamma}{\overline{\gamma}}}, \tag{1}$$

where $\overline{\gamma}$ is the average SNR of the corresponding link.

If a link experiences Rician fading, the instantaneous SNR γ follows noncentral-χ^2 distribution with PDF given as

$$f_\gamma(\gamma) = \frac{1+K}{\overline{\gamma}} \exp\Big[-K - \frac{(1+K)\gamma}{\overline{\gamma}}\Big] I_0\Big(2\sqrt{\frac{K(1+K)\gamma}{\overline{\gamma}}}\Big), \tag{2}$$

where $\overline{\gamma}$ is the average SNR of the corresponding link, K is the Rician K-factor, and $I_0(\cdot)$ is the zero-order modified Bessel function of the first kind.

III. Outage Probability Analysis

We assume that m $(m = 1, \ldots, M)$ hybrid-ARQ rounds are used to transmit the data successfully and the correct decoding of the data at the relay node occurs at round k. Therefore, if $k < m$, it indicates that the relay correctly decodes the data before the destination node, and the relay has contributed to the cooperative transmission together with the the source node for ARQ rounds $(k{+}1, \ldots, m)$. Otherwise, $k \geq m$ implies that only the source node contributes to the successful transmission of the information for this data packet round.

For hybrid-ARQ with CC scheme, the mutual information is obtained by combining received SNR over the m rounds.

The accumulated SNR $\gamma_{(m,k)}$ at the destination node after m ARQ rounds can be expressed as

$$\gamma_{(m,k)} = \sum_{i=0}^{m} \big[\gamma_{sd,i} + \gamma_{rd,i} \cdot \mathbb{1}(i > k)\big], \tag{3}$$

where $\gamma_{sd,i}$ and $\gamma_{rd,i}$ are the SNRs of the source-destination and the relay-destination links at the i-th round, respectively; and $\mathbb{1}(i > k)$ is the indicator function.

The total mutual information, $I_{(m,k)}$, after m-th round can be written according to Shannon's theorem as

$$\begin{aligned} I_{(m,k)} &= \log_2(1 + \gamma_{(m,k)}) \\ &= \log_2\Big(1 + \sum_{i=0}^{m} \big[\gamma_{sd,i} + \gamma_{rd,i} \cdot \mathbb{1}(i > k)\big]\Big). \end{aligned} \tag{4}$$

An outage after m hybrid-ARQ rounds means that the accumulated total mutual information $I_{(m,k)}$ is still less than the transmission rate R. Let $\mathrm{T_r}$ denote the earliest ARQ round after which the relay contributes the information conveyed to the destination. The outage probability $\mathrm{P_{out}}(m)$ after m ARQ transmission rounds can be expressed as [11]

$$\mathrm{P_{out}}(m) = \sum_{k=1}^{M} \Pr(I_{(m,k)} < R) \cdot \Pr(\mathrm{T_r} = k) \tag{5}$$

$$\begin{aligned} &= \Bigg[\sum_{k=1}^{m-1} \underbrace{\Pr\Big(\log_2\big(1 + \sum_{i=1}^{m} \gamma_{sd,i} + \sum_{i=k+1}^{m} \gamma_{rd,i}\big) < R\Big)}_{\mathrm{P}^{\mathrm{A}}_{\mathrm{out}}(m)} \\ &\quad + \sum_{k=m}^{M} \underbrace{\Pr\Big(\log_2\big(1 + \sum_{i=1}^{m} \gamma_{sd,i}\big) < R\Big)}_{\mathrm{P}^{\mathrm{B}}_{\mathrm{out}}(m)}\Bigg] \cdot \Pr(\mathrm{T_r} = k). \end{aligned} \tag{6}$$

To obtain the expression for $\mathrm{P_{out}}(m)$, we need to derive the solutions of $\mathrm{P}^{\mathrm{A}}_{\mathrm{out}}(m)$, $\mathrm{P}^{\mathrm{B}}_{\mathrm{out}}(m)$, and $\Pr(\mathrm{T_r} = k)$.

A. Outage Probability for Asymmetric Channel I

1) Derivation of $\mathrm{P}^{\mathrm{A}}_{\mathrm{out}}(m)$

We denote the function $\mathrm{P}^{\mathrm{A}}_{\mathrm{out}}(m)$ in (6) for the asymmetric channel I as $\mathrm{P}^{\mathrm{A}}_{\mathrm{out,I}}(m)$. It can be further expressed as follows

$$\begin{aligned} \mathrm{P}^{\mathrm{A}}_{\mathrm{out,I}}(m) &= \Pr\Big(\sum_{i=1}^{m} \gamma_{sd,i} + \sum_{i=k+1}^{m} \gamma_{rd,i} < 2^R - 1\Big) \\ &= \Pr\big(\mathcal{Y}^{(m)} + \mathcal{Z}^{(m,k)} < 2^R - 1\big) \\ &= \Pr\big(\mathcal{X}^{(m,k)} < 2^R - 1\big) = F_{\mathcal{X}^{(m,k)}}(2^R - 1), \end{aligned} \tag{7}$$

where the auxiliary variables are defined as follows: $\mathcal{Y}^{(m)} = \sum_{i=1}^{m} \gamma_{sd,i}$, $\mathcal{Z}^{(m,k)} = \sum_{i=k+1}^{m} \gamma_{rd,i}$, and $\mathcal{X}^{(m,k)} = \mathcal{Y}^{(m)} + \mathcal{Z}^{(m,k)}$; and $F_{\mathcal{X}^{(m,k)}}(\cdot)$ is the cumulative distribution function (CDF) of the random variable (RV) $\mathcal{X}^{(m,k)}$.

As $\gamma_{sd,i}$ follows the exponential distribution, its moment generating function (MGF) is expressed as $\mathcal{M}_{\gamma_{sd,i}}(s) = 1/(1 - s\overline{\gamma}_{sd})$. Then, the MGF $\mathcal{M}_{\mathcal{Y}^{(m)}}(s)$ of the RV $\mathcal{Y}^{(m)}$ is given by

$$\mathcal{M}_{\mathcal{Y}^{(m)}}(s) = \prod_{i=1}^{m} \mathcal{M}_{\gamma_{sd,i}}(s) = \frac{1}{(1 - s\overline{\gamma}_{sd})^m}. \tag{8}$$

***Remark*:** The above RV $\mathcal{Y}^{(m)} = \sum_{i=1}^{m} \gamma_{sd,i}$ is Erlang distributed as $\gamma_{sd,i}$ are independent and identically distributed (i.i.d.) exponential RVs. This can be readily shown by comparing (8) with the MGF of Erlang distribution [12, p. 67].

The RV $\gamma_{rd,i}$ is noncentral-χ^2 distributed and its MGF $\mathcal{M}_{\gamma_{rd,i}}(s)$ can be obtained from its PDF in (2) as follows

$$\mathcal{M}_{\gamma_{rd,i}}(s) = \frac{1 + K}{1 + K - s\overline{\gamma}_{rd}} \cdot \exp\Big(\frac{K \cdot \overline{\gamma}_{rd} s}{1 + K - s\overline{\gamma}_{rd}}\Big). \tag{9}$$

The RV $\mathcal{Z}^{(m,k)}$ is the sum of $(m - k)$ i.i.d. noncentral-χ^2 RVs. Its MGF $\mathcal{M}_{\mathcal{Z}^{(m,k)}}(s)$ can be expressed as

$$\begin{aligned} \mathcal{M}_{\mathcal{Z}^{(m,k)}}(s) &= \prod_{i=k+1}^{m} \mathcal{M}_{\gamma_{rd,i}}(s) \\ &= \Big[\frac{1 + K}{1 + K - s\overline{\gamma}_{rd}} \cdot \exp\Big(\frac{K \cdot s\overline{\gamma}_{rd}}{1 + K - s\overline{\gamma}_{rd}}\Big)\Big]^{m-k}. \end{aligned} \tag{10}$$

***Remark*:** Arising from the fact that a noncentral-χ^2 RV results from the sum of squares of several independent normally distributed RVs; then the sum of several noncentral-χ^2 RVs also results in a noncentral-χ^2 distributed variable. Therefore, the above RV $\mathcal{Z}^{(m,k)}$ is also noncentral-χ^2 distributed.

The MGF $\mathcal{M}_{\mathcal{X}^{(m,k)}}(s)$ of the RV $\mathcal{X}^{(m,k)}$ is expressed as

$$\begin{aligned} \mathcal{M}_{\mathcal{X}^{(m,k)}}(s) &= \mathcal{M}_{\mathcal{Y}^{(m)}}(s) \cdot \mathcal{M}_{\mathcal{Z}^{(m,k)}}(s) = (1 - s\overline{\gamma}_{sd})^{-m} \\ &\quad \cdot \Big[\frac{1 + K}{1 + K - s\overline{\gamma}_{rd}} \cdot \exp\Big(\frac{K \cdot s\overline{\gamma}_{rd}}{1 + K - s\overline{\gamma}_{rd}}\Big)\Big]^{m-k}. \end{aligned} \tag{11}$$

The CDF $F_{\mathcal{X}^{(m,k)}}(\cdot)$ of the RV $\mathcal{X}^{(m,k)}$ can be obtained from its MGF in (11) as follows

$$F_{\mathcal{X}^{(m,k)}}(x) = \mathcal{L}^{-1}\Big[\frac{1}{s} \cdot \mathcal{M}_{\mathcal{X}^{(m,k)}}(-s)\Big], \tag{12}$$

where $\mathcal{L}^{-1}[\cdot]$ represents the inverse Laplace transform.

To obtain an unified expression for $\mathrm{P}^{\mathrm{A}}_{\mathrm{out,I}}(m)$, we apply the Euler summation-based approach [13] to obtain an approximate solution for the inverse Laplace transform in (12). Then, $\mathrm{P}^{\mathrm{A}}_{\mathrm{out,I}}(m)$ is computed as

$$\begin{aligned} \mathrm{P}^{\mathrm{A}}_{\mathrm{out,I}}(m) = F_{\mathcal{X}^{(m,k)}}(2^R - 1) &= \sum_{q=0}^{Q} 2^{1-Q} \binom{Q}{q} \Bigg[\sum_{w=0}^{W+q} \frac{e^{\frac{P}{2}}(-1)^w}{\beta_w} \\ &\quad \cdot \mathrm{Re}\Bigg\{\frac{\mathcal{M}_{\mathcal{X}^{(m,k)}}\big(-\frac{P + 2\pi j w}{2 \cdot (2^R - 1)}\big)}{P + 2\pi j w}\Bigg\}\Bigg] + \varepsilon(P) + \varepsilon(W, Q), \end{aligned} \tag{13}$$

where $\mathrm{Re}\{\cdot\}$ denotes the real part of the complex number, the MGF $\mathcal{M}_{\mathcal{X}^{(m,k)}}(\cdot)$ is given in (11) and

$$\beta_w = \begin{cases} 2 & \text{if } w = 0 \\ 1 & \text{if } w = 1, \ldots, W + q, \end{cases} \tag{14}$$

and P is an arbitrary parameter controlling the discretization error $\varepsilon(P)$, which is bounded by

$$|\varepsilon(P)| \leq e^{-P}, \tag{15}$$

and the overall truncation error $\varepsilon(W,Q)$ approximates to

$$\varepsilon(W,Q) \simeq e^{\frac{P}{2}} \cdot \sum_{q=0}^{Q} 2^{1-Q}(-1)^{W+q+1}\binom{Q}{q} \cdot \mathrm{Re}\Big\{\frac{\mathcal{M}_{\mathcal{X}^{(m,k)}}\big(-\frac{P+2\pi j(W+q+1)}{2\cdot(2^R-1)}\big)}{P+2\pi j(W+q+1)}\Big\}. \quad (16)$$

***Remark*:** The exact closed-form solution for the inverse Laplace transform in (12) can be obtained in terms of higher-order derivatives from Appendix A as

$$F_{\mathcal{X}^{(m,k)}}(x) = \sum_{n=0}^{\infty}\frac{(-c)^n}{n!}\cdot\Big\{\lim_{s\to-\frac{1}{a}}\frac{d^{(m-1)}}{ds^{(m-1)}}\Big[\frac{s^{n-1}\cdot e^{sx}}{(1+bs)^{m-k+n}}\Big] + \lim_{s\to-\frac{1}{b}}\frac{d^{(m-k+n-1)}}{ds^{(m-k+n-1)}}\Big[\frac{s^{n-1}\cdot e^{sx}}{(1+as)^{m}}\Big]\Big\}+1, \quad (17)$$

where $a=\overline{\gamma}_{sd}$, $b=\overline{\gamma}_{rd}/(1+K)$, $c=K(m-k)\overline{\gamma}_{rd}/(1+K)$. There exist no universal expressions for the higher-order derivatives in (17), but they can be simply solved recursively or readily evaluated with mathematical softwares such as Mathematica and Matlab.

2) Derivation of $\mathrm{P}_{\mathrm{out}}^{\mathrm{B}}(m)$

We denote the function $\mathrm{P}_{\mathrm{out}}^{\mathrm{B}}(m)$ in (6) under the asymmetric channel I as $\mathrm{P}_{\mathrm{out,I}}^{\mathrm{B}}(m)$. It can be further expressed as

$$\mathrm{P}_{\mathrm{out,I}}^{\mathrm{B}}(m) = \Pr\Big(\sum_{i=1}^{m}\gamma_{sd,i} < 2^R-1\Big) = F_{\mathcal{Y}^{(m)}}(2^R-1), \quad (18)$$

where $F_{\mathcal{Y}^{(m)}}(\cdot)$ is the CDF of the RV $\mathcal{Y}^{(m)}=\sum_{i=1}^{m}\gamma_{sd,i}$. Since the variables $\gamma_{sd,i}$ are i.i.d. exponential RVs, then $\mathcal{Y}^{(m)}$ follows the Erlang distribution [12, p. 67]. Then, $\mathrm{P}_{\mathrm{out,I}}^{\mathrm{B}}(m)$ can be expressed from the CDF of Erlang distribution as follows

$$\mathrm{P}_{\mathrm{out,I}}^{\mathrm{B}}(m) = F_{\mathcal{Y}^{(m)}}(2^R-1) = \widetilde{\Gamma}\Big(m,\frac{2^R-1}{\overline{\gamma}_{sd}}\Big) = 1-\sum_{i=0}^{m-1}\frac{1}{i!}\Big(\frac{2^R-1}{\overline{\gamma}_{sd}}\Big)^i\cdot\exp\Big(-\frac{2^R-1}{\overline{\gamma}_{sd}}\Big), \quad (19)$$

where $\widetilde{\Gamma}(\cdot,\cdot)$ is the normalized lower incomplete Gamma function defined as $\widetilde{\Gamma}(\tau,y)=\frac{1}{\Gamma(\tau)}\int_0^y t^{\tau-1}e^{-t}\,dt$ with $\Gamma(\cdot)$ being the Gamma function; and the last equality in (19) is obtained through the power series expansion of incomplete Gamma function [14, pp. 899–902].

3) Derivation of $\Pr(\mathrm{T_r}=k)$

Let A_k denote the event that the relay is sending data to the destination at k-th ARQ round and $\overline{\mathrm{A}}_k$ stands for the event that the relay is not contributing to information transmission to the destination at k-th round yet. Then, we have the expression of $\Pr(\mathrm{T_r}=k)$ for $k=1,\ldots,M-1$ as follows

$$\begin{aligned}\Pr(\mathrm{T_r}=k) &= \Pr(\overline{\mathrm{A}}_{k-1}\cap\mathrm{A}_k)\\ &= \Pr\Big(\sum_{i=1}^{k}\gamma_{sr,i}\ge 2^R-1\Big)-\Pr\Big(\sum_{i=1}^{k-1}\gamma_{sr,i}\ge 2^R-1\Big)\\ &= \overline{F}_{\mathcal{G}^{(k)}}(2^R-1)-\overline{F}_{\mathcal{G}^{(k-1)}}(2^R-1), \end{aligned}\quad (20)$$

where $\overline{F}_{\mathcal{G}^{(k)}}(\cdot)$ is the complementary CDF of the RV $\mathcal{G}^{(k)}=\sum_{i=1}^{k}\gamma_{sr,i}$. Since $\gamma_{sr,i}$ follow exponential distribution, $\mathcal{G}^{(k)}$ is Erlang distributed [12, p. 67]. Then, we can obtain the expression for $\Pr(\mathrm{T_r}=k)$ $(k=1,\ldots,M-1)$ as

$$\begin{aligned}\Pr(\mathrm{T_r}=k) &= F_{\mathcal{G}^{(k-1)}}(2^R-1)-F_{\mathcal{G}^{(k)}}(2^R-1)\\ &= \widetilde{\Gamma}\Big(k-1,\frac{2^R-1}{\overline{\gamma}_{sr}}\Big)-\widetilde{\Gamma}\Big(k,\frac{2^R-1}{\overline{\gamma}_{sr}}\Big). \end{aligned}\quad (21)$$

For the special case of $k=M$, it means that the relay does not succeed in decoding the data in the first $(M-1)$ (re)transmission rounds, regardless the decoding result for the last ARQ round. Then, $\Pr(\mathrm{T_r}=M)$ can be expressed as

$$\begin{aligned}\Pr(\mathrm{T_r}=M) &= \Pr\Big(\mathcal{G}^{(M-1)}<2^R-1\Big)=F_{\mathcal{G}^{(M-1)}}(2^R-1)\\ &= \widetilde{\Gamma}\Big(M-1,\frac{2^R-1}{\overline{\gamma}_{sr}}\Big). \end{aligned}\quad (22)$$

Finally, substituting (13), (19), (21), and (22) into (6), we obtain the unified closed-form expression for the outage probability $\mathrm{P}_{\mathrm{out}}(m)$ under asymmetric channel I.

B. Outage Probability for Asymmetric Channel II

1) Derivation of $\mathrm{P}_{\mathrm{out}}^{\mathrm{A}}(m)$

We denote the function $\mathrm{P}_{\mathrm{out}}^{\mathrm{A}}(m)$ for the channel II as $\mathrm{P}_{\mathrm{out,II}}^{\mathrm{A}}(m)$. The variable $\mathcal{X}^{(m,k)}=\sum_{i=1}^{m}\gamma_{sd,i}+\sum_{i=k+1}^{m}\gamma_{rd,i}$ is now the sum of two Erlang distributed RVs. Utilizing the properties of Rieman-Stieltjes integral [14, pp. 608–618] and the differential relationship between CDF and PDF, we obtain the expression for $\mathrm{P}_{\mathrm{out,II}}^{\mathrm{A}}(m)$ from Appendix B as

$$\mathrm{P}_{\mathrm{out,II}}^{\mathrm{A}}(m) = 1-\exp\Big(-\frac{2^R-1}{\overline{\gamma}_{rd}}\Big)\cdot\Big[\sum_{i=0}^{m-k-1}\frac{(2^R-1)^i}{\Gamma(i+1)\cdot(\overline{\gamma}_{rd})^i} + \sum_{i=0}^{m-1}G_{2,1}^{1,1}\Big(\frac{\overline{\gamma}_{rd}\cdot\overline{\gamma}_{sd}}{(\overline{\gamma}_{rd}-\overline{\gamma}_{sd})\cdot(2^R-1)}\Big|{}^{1,m-k+i+1}_{i+1}\Big)\cdot\frac{(2^R-1)^{m-k+i}}{\Gamma(i+1)(\overline{\gamma}_{rd})^{m-k}(\overline{\gamma}_{sd})^i}\Big], \quad (23)$$

where $G_{\cdot,\cdot}^{\cdot,\cdot}(\cdot|\cdot)$ is the Meijer's G-function [14, p. 1032]. The Meijer's G function can be evaluated using Matlab.

***Remark*:** The above RV $\mathcal{X}^{(m,k)}$ is Erlang distributed only when $\overline{\gamma}_{sd}=\overline{\gamma}_{rd}$. This can be proved by showing that (23) will be in the form of (19) when $\overline{\gamma}_{sd}=\overline{\gamma}_{rd}$ holds.

2) Derivation of $\mathrm{P}_{\mathrm{out}}^{\mathrm{B}}(m)$

We denote $\mathrm{P}_{\mathrm{out}}^{\mathrm{B}}(m)$ for the channel II as $\mathrm{P}_{\mathrm{out,II}}^{\mathrm{B}}(m)$. It is straightforward to see that the RV $\mathcal{Y}^{(m)}=\sum_{i=1}^{m}\gamma_{sd,i}$ is Erlang distributed and $\mathrm{P}_{\mathrm{out,II}}^{\mathrm{B}}(m)$ is the same as $\mathrm{P}_{\mathrm{out,I}}^{\mathrm{B}}(m)$ given in (19).

3) Derivation of $\Pr(\mathrm{T_r}=k)$

The RV $\mathcal{G}^{(k)}=\sum_{i=1}^{k}\gamma_{sr,i}$ now follows the noncentral-χ^2 distribution; and its MGF is equal to $\mathcal{M}_{\mathcal{Z}^{(k,0)}}(s)$ with $\mathcal{M}_{\mathcal{Z}^{(\cdot,\cdot)}}(\cdot)$ given in (10). Using the same rationale as in Section III-A3

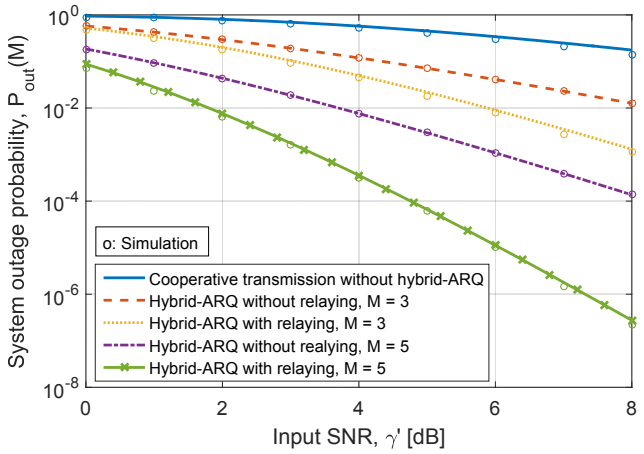

Fig. 2: System outage probability vs. input SNR for hybrid-ARQ with and without relaying in asymmetric channel I.

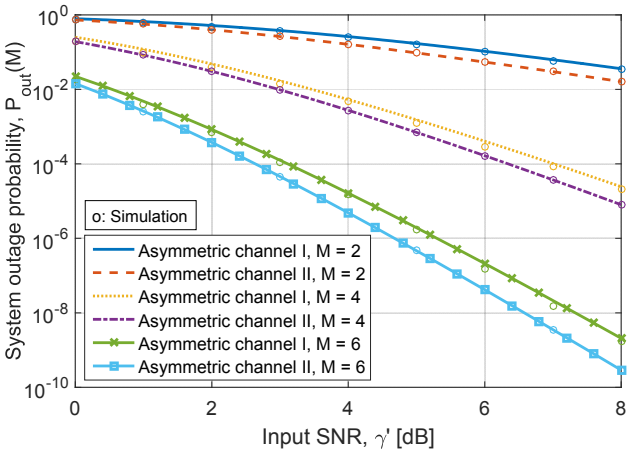

Fig. 3: System outage probability vs. input SNR for hybrid-ARQ with relaying in asymmetric channels I and II.

and skipping the derivation details, we obtain the expression for $\Pr(\mathrm{T_r} = k)$ under the asymmetric channel II as

$$\Pr(\mathrm{T_r} = k) = \begin{cases} F_{\mathcal{G}^{(k-1)}}(2^R - 1) - F_{\mathcal{G}^{(k)}}(2^R - 1) \\ \qquad\qquad \text{if } k = 1, \ldots, M-1 \\ F_{\mathcal{G}^{(M-1)}}(2^R - 1), \qquad \text{if } k = M \end{cases} \tag{24}$$

where the CDF $F_{\mathcal{G}^{(k)}}(\cdot)$ of the noncentral-χ^2 RV $\mathcal{G}^{(k)}$ is

$$F_{\mathcal{G}^{(k)}}(x) = 1 - Q_k\big(\sqrt{2kK}, \sqrt{(2(1+K)x)/\overline{\gamma}_{sr}}\big). \tag{25}$$

with $Q_k(\cdot,\cdot)$ being the Marcum Q-function [15, pp. 93–113].

Finally, substituting (23), (19), and (24) into (6), we obtain the exact expression of $\mathrm{P_{out}}(m)$ under asymmetric channel II.

IV. Delay-Limited Throughput Analysis

A widely used performance metric for throughput analysis is the DL throughput $\overline{G}_{DL}$, which is expressed as [4]

$$\begin{aligned} \overline{G}_{DL}(R, M) &= \sum_{m=1}^{M} \frac{R}{m}\big[\mathrm{P_{out}}(m-1) - \mathrm{P_{out}}(m)\big] \\ &= R \cdot \Big[1 - \sum_{m=1}^{M-1} \frac{\mathrm{P_{out}}(m)}{m(m+1)} - \frac{\mathrm{P_{out}}(M)}{M}\Big]. \end{aligned} \tag{26}$$

An advantage of the DL throughput lies in its ability to track slow time variations in the channel, which does not resort to the long-time behavior.

V. Numerical Results

In this section, the analytical expressions presented in the previous sections are evaluated numerically and validated using simulations. We assume the following simulation parameters for the results presented in this section, unless otherwise stated: the source and the relay transmit with the same power, i.e., $P_s = P_r$. The mean values of the fading taken into account path loss and shadowing is $|h_{sd}|^2 = |h_{sr}|^2 = |h_{rd}|^2 = 0.5$. The transmission rate R is $2\,\mathrm{bps/Hz}$ unless otherwise stated. The Rician K-factor for the LoS link is set to 2.

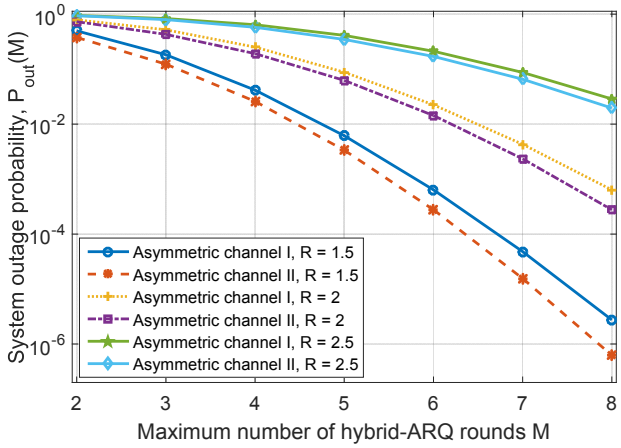

Fig. 4: System outage probability vs. maximum hybrid-ARQ transmission rounds M in asymmetric channels I and II.

Figure 2 shows the system outage probability $P_{out}(M)$ with different relaying and ARQ configurations in the asymmetric channel I. It can be seen that hybrid-ARQ greatly decrease the outage probability and hybrid-ARQ with relaying further improves the performance. At the system outage probability of 10^{-2} with $M = 3$, the performance difference for hybrid-ARQ schemes with and without relaying can be as large as around 2 dB. Also, the realized gain due to relaying increases as the maximum number of transmission rounds, M, grows.

Figures 3, 4 and 5 compare the system outage performance of the investigated asymmetric channels. It is found that the asymmetric channel II has better outage performance than that of the channel I. This difference is explained by the fact that the presence of LoS for the source-relay link in channel II ensures that statistically the relay correctly decodes the data faster than in scenario I; therefore, greater gain can be achieved from the cooperative transmission of both source and relay under the same delay constraint. This potentially implies that while there is no direct link between the source

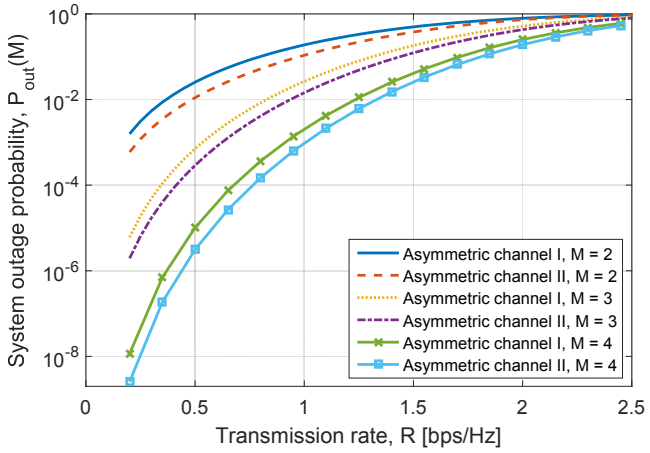

Fig. 5: System outage probability vs. transmission rate R for hybird-ARQ with relaying at input SNR $\gamma' = 0\,\mathrm{dB}$.

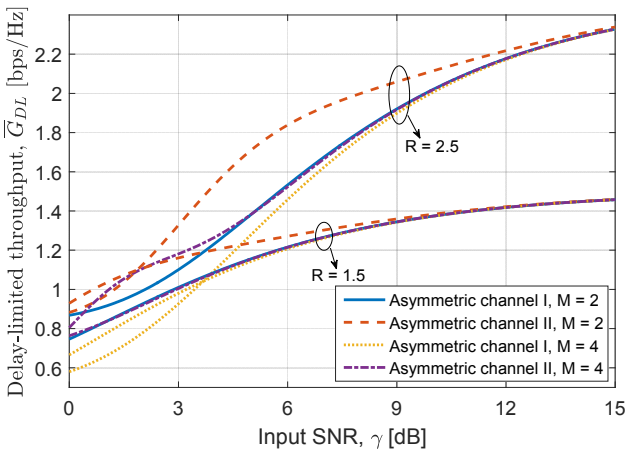

Fig. 6: Delay-limited throughput vs. input SNR in asymmetric channels I and II for different values of M and R.

and destination, the relay should be placed closer to the source to achieve better outage performance. However, this performance difference between the two asymmetric channels narrows as the maximum transmission rounds M increases or the transmission rate R decreases, as can be seen from Fig. 4 and Fig. 5.

Figure 6 on the next page depicts the DL throughput versus SNR for varying maximum transmission rounds M and transmission rate R. For low SNR values, it is found that the DL throughput decreases as the maximum transmission rounds M increases, this is the cost of achieving lower outage probability. However, the difference is negligible for large SNR values, which implies that the current R is small for the value of M and the SNR such that it becomes a limit factor for achieving greater throughput. Meanwhile, for the same value of M, the throughput decreases as the rate increases for low SNR values, while the opposite is true for large SNR values. Optimization of the transmission rate has been investigated for other scenarios in [3], [5] and is without the scope of this paper.

VI. Conclusion

In this paper, we studied the performance of relay-ARQ networks with delay constraint over asymmetric fading channels. We consider a fast-fading channel, where the fading varies independently from one hybrid-ARQ round to another. The delay-limited throughput and the system outage probability were derived and analyzed. Supported by our results, we can reconfirm that the system with combined deployment of relaying and hybrid-ARQ outperforms those with only one of the above techniques or none of them implemented also in the investigated asymmetric fading channels. Significant performance improvement is achieved by increasing the number of ARQ-based retransmissions. The results show that the performance is significantly better when the relay is in LoS condition with respect to the source rather than to the destination. The derived results are validated by Monte Carlo simulations.

Appendix A
Derivation of the solution (17) in Section III-A1

To obtain the exact solution for $\mathrm{P}^{\mathrm{A}}_{\mathrm{out,I}}(m)$ in (17), we first express the exponential function in (11) in series using $e^x = \sum_{n=0}^{\infty} x^n/n!$ and make the following change of variables for the sake of notational simplicity: $\overline{\gamma}_{sd} \to a$, $\overline{\gamma}_{rd}/(1+K) \to b$, $K(m-k)\overline{\gamma}_{rd}/(1+K) \to c$, then the inverse Laplace transform (12) can be written as

$$F_{\mathcal{X}^{(m,k)}}(x) = \sum_{n=1}^{\infty} \frac{(-c)^n}{n!} \underbrace{\mathcal{L}^{-1}\Big[\frac{s^{n-1}}{(1+as)^m(1+bs)^{m-k+n}}\Big]}_{\mathcal{I}_1(x;n)} + \underbrace{\mathcal{L}^{-1}\Big[\frac{1}{s(1+as)^m(1+bs)^{m-k}}\Big]}_{\mathcal{I}_2(x)}. \tag{27}$$

Next, we express the inverse Laplace transform term $\mathcal{I}_1$ with the contour integral and Bromwich's integral [16, pp. 42–45] as follows

$$\mathcal{I}_1(x;n) = \frac{1}{2\pi j}\oint_{c-\infty j}^{c+\infty j} \underbrace{\frac{s^{n-1}\cdot e^{sx}}{(1+as)^m(1+bs)^{m-k+n}}}_{F_s(s)} ds = \frac{1}{2\pi j}\oint_C F_s(s)\,ds - \int_{C_R} F_s(s)\,ds, \tag{28}$$

where C_R is a semicircle of infinite circle in the left half of the s-plane and C is the closed contour including C_R and Bromwich's contour. With this choice of the closed contour and using Jordan's lemma [16, pp. 29–30], the second integral in (28) is forced to zero, and $\mathcal{I}_1(x;n)$ simply equals the integral along the closed contour. Within the closed contour in the left half-plane, there exists a pole of m-th order at $s = -1/a$ and a pole of $(m-k+n)$-th order at $s = -1/b$. Next, using Cauchy's residue theorem [16, pp. 9–12], we can obtain

$$\mathcal{I}_1(x;n) = \mathrm{Res}\Big[F_s(s); -\frac{1}{a}\Big] + \mathrm{Res}\Big[F_s(s); -\frac{1}{b}\Big], \tag{29}$$

where the residues are calculated as follows

$$\mathrm{Res}\Big[F_s(s);-\frac{1}{a}\Big]=\lim_{s\to-\frac{1}{a}}\frac{d^{(m-1)}}{ds^{(m-1)}}\Big[\frac{s^{n-1}\cdot e^{sx}}{(1+bs)^{m-k+n}}\Big], \quad (30)$$

$$\mathrm{Res}\Big[F_s(s);-\frac{1}{b}\Big]=\lim_{s\to-\frac{1}{b}}\frac{d^{(m-k+n-1)}}{ds^{(m-k+n-1)}}\Big[\frac{s^{n-1}\cdot e^{sx}}{(1+as)^{m}}\Big]. \quad (31)$$

Using the same rationale, the inverse Laplace transform $\mathcal{I}_2(x)$ can be expressed as

$$\mathcal{I}_2(x)=\lim_{s\to-\frac{1}{b}}\frac{d^{(m-k-1)}}{ds^{(m-k-1)}}\Big[\frac{e^{sx}}{s(1+as)^{m}}\Big] + \lim_{s\to-\frac{1}{a}}\frac{d^{(m-1)}}{ds^{(m-1)}}\Big[\frac{e^{sx}}{s(1+bs)^{m-k}}\Big]+1. \quad (32)$$

By comparing (30), (31) and (32), it can be seen that the following relationship holds: $\mathcal{I}_2(x)=\mathcal{I}_1(x;n=0)+1$. Therefore, the CDF $F_{\mathcal{X}^{(m,k)}}(x)$ can be expressed as

$$F_{\mathcal{X}^{(m,k)}}(x)=\sum_{n=0}^{\infty}\frac{(-c)^n}{n!}\cdot\mathcal{I}_1(x;n)+1. \quad (33)$$

Finally, substituting (29)–(31) into (33), we obtain the exact expression for $F_{\mathcal{X}^{(m,k)}}(x)$ as shown in (17).

Appendix B
Derivation of $\mathrm{P}^{\mathrm{A}}_{\mathrm{out,II}}(m)$ in Section III-B1

We first derive the CDF $F_{\mathcal{X}^{(m,k)}}(x)$ of the RV $\mathcal{X}^{(m,k)}=\mathcal{Y}^{(m)}+\mathcal{Z}^{(m,k)}$, where $\mathcal{Y}^{(m)}=\sum_{i=1}^{m}\gamma_{sd,i}$ and $\mathcal{Z}^{(m,k)}=\sum_{i=k+1}^{m}\gamma_{rd,i}$ are two independent Erlang distributed RVs. Since an Erlang distributed RV is defined only on the positive half-axis, the CDF $F_{\mathcal{X}^{(m,k)}}(x)$ can be computed as follows

$$F_{\mathcal{X}^{(m,k)}}(x)=\int_0^x f_{\mathcal{Z}^{(m,k)}}(z)\cdot F_{\mathcal{Y}^{(m)}}(x-z)\,dz=\int_0^x f_{\mathcal{Z}^{(m,k)}}(z)\cdot\Big[1-\sum_{i=0}^{m-1}\frac{1}{i!}\Big(\frac{x-z}{\overline{\gamma}_{sd}}\Big)^i\exp\Big(\frac{z-x}{\overline{\gamma}_{sd}}\Big)\Big]\cdot dz=\underbrace{\int_0^x f_{\mathcal{Z}^{(m,k)}}(z)\,dz}_{\mathcal{I}_a} - \underbrace{\int_0^x\sum_{i=0}^{m-1}\frac{1}{i!}\Big(\frac{x-z}{\overline{\gamma}_{sd}}\Big)^i\exp\Big(-\frac{x-z}{\overline{\gamma}_{sd}}\Big)\cdot f_{\mathcal{Z}^{(m,k)}}(z)\,dz}_{\mathcal{I}_b}. \quad (34)$$

Then, $\mathcal{I}_a$ and $\mathcal{I}_b$ can be calculated as follows

$$\mathcal{I}_a=F_{\mathcal{Z}^{(m,k)}}(x)=1-\sum_{i=0}^{m-k-1}\frac{1}{i!}\Big(\frac{x}{\overline{\gamma}_{rd}}\Big)^i\exp\Big(-\frac{x}{\overline{\gamma}_{rd}}\Big), \quad (35)$$

and

$$\mathcal{I}_b=\sum_{i=0}^{m-1}\frac{\exp\big(-\frac{x}{\overline{\gamma}_{sd}}\big)}{i!\Gamma(m-k)(\overline{\gamma}_{sd})^i(\overline{\gamma}_{rd})^{m-k}}\cdot\underbrace{\int_0^x(x-z)^i\exp\Big(\frac{\overline{\gamma}_{rd}-\overline{\gamma}_{sd}}{\overline{\gamma}_{sd}\cdot\overline{\gamma}_{rd}}\cdot z\Big)\cdot z^{m-k-1}\,dz}_{\mathcal{I}_c}. \quad (36)$$

The integral $\mathcal{I}_c$ is in the form of $\int_0^{\omega}t^{\alpha-1}e^{\lambda t}(\omega-t)^{\rho-1}\,dt$. Employing the properties of confluent hypergeometric function and its relationship with the Meijer's G-function [14, pp. 347, 1023, 1035], the integral can be solved, after some algebraic manipulations, in terms of Meijer's G-function as

$$\int_0^{\omega}t^{\alpha-1}e^{\lambda t}(\omega-t)^{\rho-1}\,dt=\frac{\Gamma(\alpha)\cdot\omega^{\alpha+\rho-1}}{e^{-\lambda\omega}}\cdot G_{2,1}^{1,1}\Big(\frac{1}{\lambda\omega}\Big|\begin{smallmatrix}1,\alpha+\rho\\ \rho\end{smallmatrix}\Big). \quad (37)$$

Making the following changes of random variables: $\omega\to x$, $t\to z$, $\alpha\to m-k$, $\lambda\to(\overline{\gamma}_{rd}-\overline{\gamma}_{sd})/(\overline{\gamma}_{sd}\cdot\overline{\gamma}_{rd})$, $\rho\to i+1$; then the integral $\mathcal{I}_c$ in (36) can be expressed as

$$\mathcal{I}_c=\frac{\Gamma(m-k)\cdot x^{m-k+i}}{\exp\Big(\frac{(\overline{\gamma}_{sd}-\overline{\gamma}_{rd})\cdot x}{\overline{\gamma}_{sd}\cdot\overline{\gamma}_{rd}}\Big)}\cdot G_{2,1}^{1,1}\Big(\frac{\overline{\gamma}_{rd}\cdot\overline{\gamma}_{sd}}{(\overline{\gamma}_{rd}-\overline{\gamma}_{sd})\cdot x}\Big|\begin{smallmatrix}1,m-k+i+1\\ i+1\end{smallmatrix}\Big). \quad (38)$$

Substituting (35)-(38) into (34), we obtain the expression for $F_{\mathcal{X}^{(m,k)}}(x)$. Consequently, the expression of $\mathrm{P}^{\mathrm{A}}_{\mathrm{out,II}}(m)=F_{\mathcal{X}^{(m,k)}}(2^R-1)$ can be obtained as shown in (23).

Acknowledgment

We gratefully acknowledge the Regional Research Fund of Norway (RFF) for supporting our research.

References

[1] A. Nosratinia, T. E. Hunter, and A. Hedayat, "Cooperative communication in wireless networks," *IEEE Commun. Mag.*, vol. 42, no. 10, pp. 74–80, Oct. 2004.

[2] E. Dahlman, S. Parkvall, and J. Skold, *4G: LTE/LTE-Advanced for Mobile Broadband*, 2nd ed. Academic press, 2014.

[3] R. Narasimhan, "Throughput-delay performance of half-duplex hybrid-ARQ relay channels," in *Proc. of IEEE Int. Conf. Commun. (ICC)*, May 2008, pp. 986–990.

[4] B. Maham, A. Behnad, and M. Debbah, "Analysis of outage probability and throughput for half-duplex hybrid-ARQ relay channels," *IEEE Trans. Veh. Technol.*, vol. 61, no. 7, pp. 3061–3070, Sept. 2012.

[5] B. Makki, T. Eriksson, and T. Svensson, "On the performance of the relay-ARQ networks," *IEEE Trans. Veh. Technol.*, no. 99, Apr. 2016.

[6] B. Makki and T. Eriksson, "On the performance of MIMO-ARQ systems with channel state information at the receiver," *IEEE Trans. Commun.*, vol. 62, no. 5, pp. 1588–1603, May 2014.

[7] J. Li, B. Makki, and T. Svensson, "Performance analysis and cooperation mode switch in HARQ-based relaying," in *Proc. of IEEE GlobeCom Workshops (GC Wkshps)*, Dec. 2014, pp. 930–935.

[8] J. Ouyang, M. Lin, and Y. Zhuang, "Performance analysis of beamforming with feedback delay in two-hop AF relaying over Rayleigh-Rician fading channels," *Electron. Lett.*, vol. 48, no. 11, pp. 663–665, May 2012.

[9] S. S. Soliman and N. C. Beaulieu, "Dual-hop AF relaying systems in mixed Nakagami-m and Rician links," in *Proc. of IEEE GlobeCom Workshops (GC Wkshps)*, Dec. 2012, pp. 447–452.

[10] N. Kapucu, M. Bilim, and I. Develi, "Outage probability analysis of dual-hop decode-and-forward relaying over mixed Rayleigh and generalized Gamma fading channels," *Wireless Pers. Commun.*, vol. 71, no. 2, pp. 947–954, Jul. 2013.

[11] T. Tabet, S. Dusad, and R. Knopp, "Diversity-multiplexing-delay tradeoff in half-duplex ARQ relay channels," *IEEE Trans. Inf. Theory*, vol. 53, no. 10, pp. 3797–3805, Oct. 2007.

[12] S. Miller and D. Childers, *Probability and Random Processes: with Applications to Signal Processing and Communications*. Elsevier, 2004.

[13] J. Abate and W. Whitt, "Numerical inversion of Laplace transforms of probability distributions," *ORSA Journal on Computing*, vol. 7, no. 1, pp. 36–43, Feb. 1995.

[14] A. Jeffrey and D. Zwillinger, *Table of Integrals, Series, and Products*, 7th ed. Elsevier, 2007.

[15] M. K. Simon and M.-S. Alouini, *Digital Communication over Fading Channels*. John Wiley & Sons, 2005.

[16] D. G. Duffy, *Greens Functions with Applications*. CRC Press, 2015.